

**MASTER M2  
UE QUESTIONS D'ACTUALITÉ EN BIOLOGIE CELLULAIRE  
SESSION DE DECEMBRE 2008**

**Durée de l'épreuve : 3 heures.**

Le sujet porte sur l'article ci-joint de Pouthas *et al.* paru dans la revue Journal of Cell Science en Juin 2008 (vol 121, p2406-2414) ; les données « Supplementary data » ne sont pas fournies, n'étant pas indispensables à la compréhension de l'article.

- 1) Rédigez un résumé de l'article en moins de 300 mots (indiquez le nombre de mots utilisés à la fin) et proposer 5 mots-clés. (6 points)
- 2) Représentez en schéma et décrivez le mécanisme par lequel la fibronectine exerce ses effets (2 points)
- 3) Décrivez les principaux résultats et conclusions de la figure 1 (masqués dans cette version) (3 points)
- 4) Quels autres marqueurs auraient pu être utilisés dans cette étude pour visualiser les zones de contact avec le substrat ? (2 points)
- 5) Qu'apporte la vidéomicroscopie (ou time-lapse) dans cette étude ? (2 points)
- 6) Il existe de nombreux exemples de migration cellulaire in vivo. Expliquez le choix de ce système particulier par les auteurs. Quel(s) paramètres sont mieux pris en compte par rapport à la culture cellulaire ? (3 points)
- 7) Que permet de visualiser la claudin-GFP chez le poisson-zèbre ? (1 point)
- 8) Comment met-on en œuvre un test de « wound-healing » in vitro ? (1 point)

# In migrating cells, the Golgi complex and the position of the centrosome depend on geometrical constraints of the substratum

François Pouthas, Philippe Girard, Virginie Lecaudey, Thi Bach Nga Ly, Darren Gilmour, Christian Boulin, Rainer Pepperkok and Emmanuel G. Reynaud\*

Cell Biology and Cell Biophysics Programme, European Molecular Biology Laboratory (EMBL), Meyerhofstrasse 1, 69117 Heidelberg, Germany

\*Author for correspondence (e-mail: reynaud@embl.de)

Accepted 9 April 2008

*Journal of Cell Science* 121, 2406-2414 Published by The Company of Biologists 2008  
doi:10.1242/jcs.026849

## Summary

## Introduction

The migration of mammalian cells is typically initiated by a morphological polarization that is characterized by the formation of a leading edge at the front of the cell (lamellipod). Adhesion receptors on this membrane extension bind to ligands on the underlying substratum, allowing conversion of mechanical forces into cellular locomotion. Following lamellipod extension, the cytoskeleton contracts until the cell breaks adhesion points that attach the uropod to the substrate (Li et al., 2005). In addition, it has been proposed that cell polarization leads to the reorientation of the Golgi complex and the microtubule-organizing centre (MTOC) towards the leading edge (Nabi, 1999). This change in position is driven by the same proteins that regulate cell polarity, e.g. by Cdc42 (Itoh et al., 2002). Cdc42-induced MTOC orientation contributes to polarized migration by facilitating microtubule growth into the lamella- and microtubule-mediated delivery of Golgi-derived vesicles to the leading edge, which provides membrane and associated proteins needed for forward protrusion (Etienne-Manneville and Hall, 2002; Etienne-Manneville, 2004). Indeed, many migrating cell types, such as fibroblasts, neurons or macrophages, reorient the Golgi complex and the MTOC towards the leading edge during migration in 2D culture (Nemere et al., 1985; Magdalena et al., 2003; Schaar and McConnell, 2005). This reorientation also occurs during wound healing (Euteneuer and Schliwa, 1992), tubulogenesis (Yu et al., 2003), electrical stimulation (Pu and Zhao, 2005), shear stress (Coan et al., 1993) and early development (Carney and Couve, 1989).

This observation has led to a model in which Golgi and/or MTOC repositioning are thought to always lead to a final front position of these two organelles. However, mixed front-back positions have been observed in CHO cells during wound healing (Yvon et al., 2002), in endothelial cells under shear stress (Coan et al., 1993) and in fibroblasts grown on grooved substrates or grown in collagen gels (Schütze et al., 1991). These results challenge the view that the Golgi complex – similar to the centrosome – is always at the leading edge of a migratory cell. Interestingly, when considering migrating cells *in vivo*, e.g. T-cell lymphocytes, they always migrate with the Golgi complex and the centrosome at the back of the cell in the uropod, and reorient themselves only when binding to their target cell (Kupfer et al., 1985; Serrador et al., 1999; Ratner et al., 1997). This rear position, in respect to the nucleus, of these two organelles has also been observed *in vitro*: during the migration of kangaroo rat kidney (Ptk2) cells following stimulation with hepatocyte growth factor (HGF) (Danowski et al., 2001), during the migration of erythroleukemia cells by following stimulation with phorbol myristate acetate (PMA) and during developmental processes such as the ingression of primary mesenchyme cells in sea urchin (Anstrom and Raff, 1988). It appears from these different studies that the factors that determine the position of the Golgi complex are still entirely unclear.

In this study, we have mimicked the *in-vivo* situation in which cells do not migrate freely but under high geometrical constraints by using micropatterned lines of fibronectin. This environment mimics the partial orientation of extracellular matrix (ECM) fibres

that occur within tissue that have been shown to precisely control cell shape and length (Levina et al., 2001), directionality of cell migration (Parker et al., 2002) and adhesion (Lehnert et al., 2004). Using this simple system, we demonstrate that linear geometrical constraints leads to cell polarization, displacement of the Golgi complex from its juxtannuclear position, and to the rearward localization of the Golgi complex and the centrosome. We confirmed this phenomenon *in vivo* using the well-defined migrating lateral line primordium (llp) of the zebrafish. Our study demonstrates that geometrical constraint is a very important factor, which determines the positions of the Golgi complex and the centrosome within a cell during migration.

## Results

**Cells elongate and polarize along a linear pattern of fibronectin**  
Two cell lines, Ptk2 cells and the African green monkey kidney cell line Bsc1, were cultured on micropatterned surfaces, alternating cell-adhesive strips (fibronectin, FN) and cell-repulsive strips poly(L-lysine)-*g*-poly(ethylene glycol) (PLL-*g*-PEG), both 6  $\mu\text{m}$  in width (Fig. 1A). Under these growth conditions, Bsc1 cells show a higher degree of elongation and polarization when compared with non-patterned cells (Fig. 1B,C). Ptk2 cells, which spanned more than one line, also elongate and polarize (Fig. 1D). We quantitatively analysed this increase of cellular polarization by calculating the deformation index (DI), which is based on the ratio between the major axis and the minor axis of the ellipse that defines the best cell-edge fit when comparing patterned with non-patterned cell growth conditions. A perfectly circular cell corresponds to  $\text{DI}=0$ , and the DI increases as the cell polarizes. Contours of cells were determined and centred (Fig. 1E), then aligned along their major axis (Fig. 1F), projected and demarcated (Fig. 1G and see supplementary material Fig. S1). The major and minor axes that were obtained reflect the general morphology of a cell population.

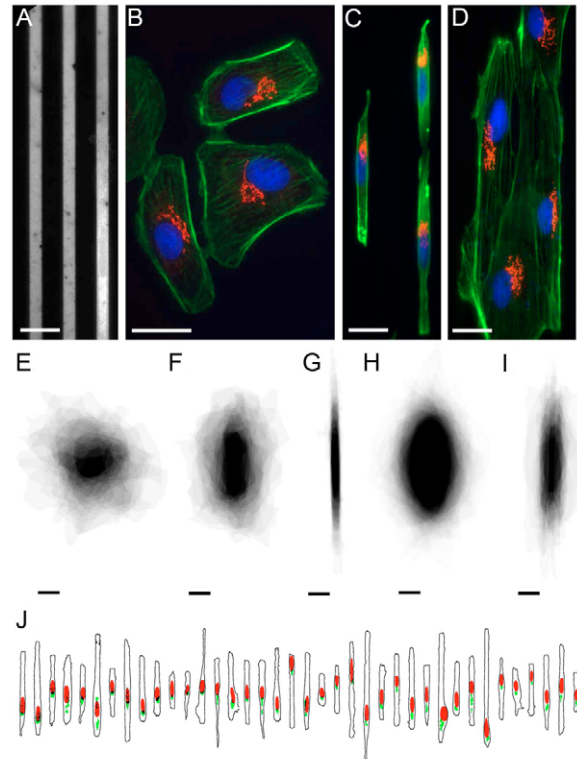


**Fig. 1.** Cells on fibronectin-patterned lines are polarized. (A) Patterned, 6- $\mu\text{m}$  thick fibronectin lines and PLL-*g*-PEG. (B) Bsc1 cells on a standard glass coverslip labelled for the actin network (green), the Golgi complex (red) and the nucleus (blue). (C) Bsc1 cells labelled as in B, grown on 6- $\mu\text{m}$  fibronectin lines. (D) Ptk2 cells labelled as in B, grown on 6- $\mu\text{m}$  fibronectin lines. (E) Centered projection of 100 Bsc1 cells grown on a standard coverslip demarcated to outline the mean cell size and shape, scale bar 10  $\mu\text{m}$  (see supplementary material Fig. S1). (F) Centered and aligned (along the longest cell axis) projection of 100 Bsc1 cells grown on a standard coverslip (see supplementary material Fig. S1). (G) Centered and aligned (along the longest cell axis) projection of 100 Bsc1 cells grown on fibronectin line (see supplementary material Fig. S1). (H) Centered and aligned (along the longest cell axis) overlay of 50 Ptk2 cells grown on a standard coverslip (see supplementary material Fig. S1). (I) Centered and aligned (along the longest cell axis) overlay of 50 Ptk2 cells grown on fibronectin line (see supplementary material Fig. S1). (J) Threshold images of 38 Bsc1 cells grown on 6- $\mu\text{m}$  fibronectin lines, fixed and analysed by immunofluorescence. Actin cell contour (black, phalloidin staining), nucleus (red, Hoechst staining) and Golgi (green, GM130 staining). Scale bars, 20  $\mu\text{m}$  (A-D); 10  $\mu\text{m}$  (E-I).

investigated the relative positions of the nucleus and the Golgi complex. We developed a plugin under ImageJ (National Institutes of Health, Bethesda, MD) allowing us to measure statistically the displacement of the Golgi complex from the nucleus (supplementary material Fig. S2). In brief, nuclear and Golgi complex surface and contours were calculated and projected. The distance and angle between the nucleus border and every single pixel defining the Golgi complex was measured. The results are plotted using a box plot representation where *y* is the distance of the nuclear border (o) to the Golgi complex in micrometer. The box illustrates the average spreading of the Golgi as well as the maximum and minimum distance between the nuclear envelope and the Golgi complex. We compared the Bsc1 cells that aligned along one single fibronectin line, and Ptk2 cells that spread over more than one line. Both cell types grown onto FN lines show a displacement of the Golgi

Cells displace their Golgi complex from the nucleus when grown on a linear pattern of fibronectin

As we observed an unusual displacement of the Golgi complex from its classical juxtannuclear area in cells grown on FN lines, we

**Table 1. Characteristics of Bsc1 and Ptk2 cells grown on 6- $\mu$ m fibronectin lines**

|            |    | Events | Major          | Minor           | Major/Minor     | DI value |
|------------|----|--------|----------------|-----------------|-----------------|----------|
| Bsc1 cells |    |        |                |                 |                 |          |
| Cell       | NP | 100    | 94 $\pm$ 26    | 53 $\pm$ 20     | 1.94 $\pm$ 0.76 | 0.27     |
|            | P  | 57     | 122 $\pm$ 38.5 | 9.1 $\pm$ 1.5   | 13.8 $\pm$ 5.1  | 0.86     |
| Nuc        | NP | 100    | 21.3 $\pm$ 4.4 | 15.0 $\pm$ 3.6  | 1.45 $\pm$ 0.25 | 0.17     |
|            | P  | 61     | 24.9 $\pm$ 4.4 | 7.0 $\pm$ 1.2   | 3.65 $\pm$ 0.99 | 0.56     |
| Ptk2 cells |    |        |                |                 |                 |          |
| Cell       | NP | 150    | 103 $\pm$ 31   | 54 $\pm$ 20     | 2.05 $\pm$ 0.78 | 0.31     |
|            | P  | 35     | 130 $\pm$ 32   | 26 $\pm$ 12     | 6.91 $\pm$ 7.2  | 0.66     |
| Nuc        | NP | 147    | 19.4 $\pm$ 2.9 | 15.0 $\pm$ 2.65 | 1.31 $\pm$ 0.20 | 0.12     |
|            | P  | 62     | 20.2 $\pm$ 4.0 | 10.7 $\pm$ 2.8  | 2.01 $\pm$ 0.73 | 0.30     |

NP, non-patterned; P, patterned.

complex from the nucleus in comparison to non-patterned growth conditions (Fig. 2A,B). 40% of Bsc1 cells have a displaced Golgi under patterned conditions as opposed to 5% in the normal non-patterned growth conditions (Fig. 2A,B) with a maximal distance of 11  $\mu$ m. However, only 20% of Ptk2 cells showed a displaced Golgi (Fig. 2C,D) but with a displacement of up to 20  $\mu$ m. In conclusion, cells growing on a linear pattern show a striking displacement of the Golgi complex compared with cells grown on patterned lines (Fig. 2E).

During cell migration the Golgi complex is positioned behind the nucleus

We performed time-lapse experiments to find out whether the displacement of the Golgi complex is a permanent or transient phenomenon. Given the higher number of GA displacement, we chose the Bsc1 cell line for this analysis. Moreover, their polarized phenotype was more often restricted to a single fibronectin line even if a lower fraction of cells (10 to 15%, data not shown) could be observed spanning up to three lines. Bsc1 are highly motile cells on FN patterned lines (supplementary material Movie 1). Time-lapse video microscopy showed that polarized cells elongate on the FN strips thereby forming an extended but restricted lamellipod and a shorter tail. Interestingly, we could distinguish two cell motility behaviours, a fast movement (46 $\pm$ 10  $\mu$ m/minute) of small cells with very pronounced anterior ruffles and short tails (Fig. 3A) and a slow movement (0.9 $\pm$ 0.4  $\mu$ m/minute) of long cells with elongated processes (Fig. 3B). The result were short cells and long extended cells, respectively. We transfected them with a nuclear marker

(H2b-HcRed) and a Golgi marker (GFP<sup>2</sup>-GalT) in order to follow both organelles during migration, and observed that the Golgi complex position varies during cell migration in extended cells (Fig. 3C,D, supplementary material Fig. S3, Movie 2). Surprisingly, in the majority of cases, the Golgi complex was located behind the nucleus with respect to the direction of migration. We therefore performed a statistical analysis of the position of the Golgi complex in those cells by immunofluorescence using an actin marker (Alexa-Fluor-488 conjugated to phalloidin) to identify the migrating edge. The Golgi complex was located behind the nucleus in 70% of the cells, in the middle in 10% and in the front in 20% (Table 2). Cells grown on FN lines usually restrict themselves to one single line for migration. However, early after plating we observed that a fraction of the cells (usually 10%) migrated by using more than one line to extend their lamellipod; later on, because more lines were occupied, cells only used one line to migrate. We took advantage of this observation to analyse cells that used two or three lines to extend their lamellipod as well as cells patterned on fibronectin lines of different strip widths (6  $\mu$ m, 14  $\mu$ m, 20  $\mu$ m, 25  $\mu$ m, 30  $\mu$ m and 40  $\mu$ m). Whereas 70% of the cells migrating on a single 6- $\mu$ m FN line have the Golgi behind the nucleus, their number decreases to 30% when cells migrate on larger strips (Table 2). The intermediate localization (juxtannuclear) increases from 10% to 25%, whereas the front localization is observed in 20% to 50%. This shows a clear correlation between the width of the migrating path and the positioning of the Golgi complex. Interestingly, the rear location is minimal at 30%.

These results clearly indicate that the Golgi complex localizes mainly behind the nucleus in Bsc1 cells that migrate on thin linear

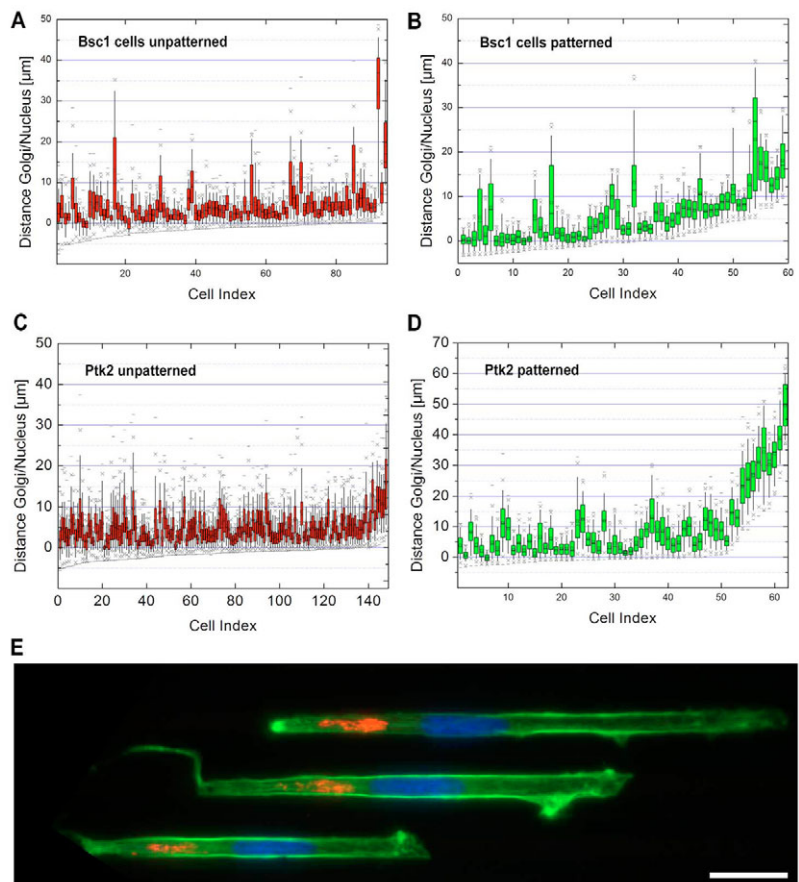


**Fig. 2.** The Golgi complex is displaced on patterned cells. (A) Distance between the border of the nucleus (0) and the Golgi complex (red box) in Bsc1 cells grown on a standard coverslip. (B) Distance between the border of the nucleus (0) and the Golgi complex (green box) in Bsc1 cells grown on 6  $\mu$ m fibronectin lines. (C) Distance between the border of the nucleus (0) and the Golgi complex (red box) in Ptk2 cells grown on a standard coverslip. (D) Distance between the border of the nucleus (0) and the Golgi complex (green box) in Ptk2 cells grown on 6- $\mu$ m fibronectin lines. (E) Bsc1 cells grown on 6- $\mu$ m fibronectin lines labelled for the actin network (green), the Golgi complex (red) and the nucleus (blue). Scale bar, 20  $\mu$ m.

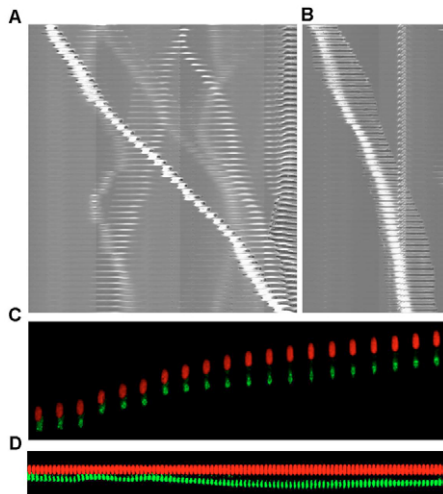


**Fig. 3.** Migration leads to displacement of the Golgi complex. (A) Montage of the fast-migrating Bsc1 cell on a 6- $\mu\text{m}$  fibronectin line (1 image/15 minutes; total time, 12.5 hours). (B) Montage of a slow-migrating Bsc1 cell on a 6- $\mu\text{m}$  fibronectin line (1 image/15 minutes; total time, 12.25 hours). (C) Montage of a migrating Bsc1 cell, nucleus (H2B-HcRed), Golgi complex (GFP<sup>2</sup>-GalT) (1 image/30 minutes; total time, 10 hours). (D) Montage of a migrating Bsc1 cell centred on the nucleus (H2B-HcRed), Golgi complex (GalT-GFP<sup>2</sup>) (1 image/5 minutes; total time, 8.5 hours).

patterns. The larger the migrating path, the more often the Golgi is located ahead of the nucleus. This clearly shows that the position of the Golgi complex directly depends on the geometrical constraints imposed to the migrating cells.

#### The rearward position of the Golgi complex is maintained during directional changes

Using video microscopy, we then investigated the Golgi complex positioning when cells switch their migration direction. We followed 39 cells that had been transfected with a nuclear marker and a Golgi marker. Of those cells, 35 showed a rear location of the Golgi complex, two a middle position and two a front position of the Golgi complex (Fig. 4A). Migrating cells follow a persistent random walk movement defined by both cell speed and directional persistence time. Persistence characterizes the average time between significant changes in the direction of migration (Dunn, 1983; Gail and Boone, 1970; Othmer et al., 1988). However, in our cases, as cells followed the fibronectin line, the persistence time is very long because the cells change direction only when encountering another cell that moves in the opposite direction, or when reaching the end of the line (Fig. 4C-E, supplementary material Movie 3). This occurs in 15 out of 39 cells. Regardless of whether the Golgi complex was initially positioned behind ( $n=11$ ), in the perinuclear region ( $n=3$ ) or in front of the cell ( $n=1$ ), the Golgi relocates at the rear after directional change (Fig. 4B). Therefore, we conclude that the rear

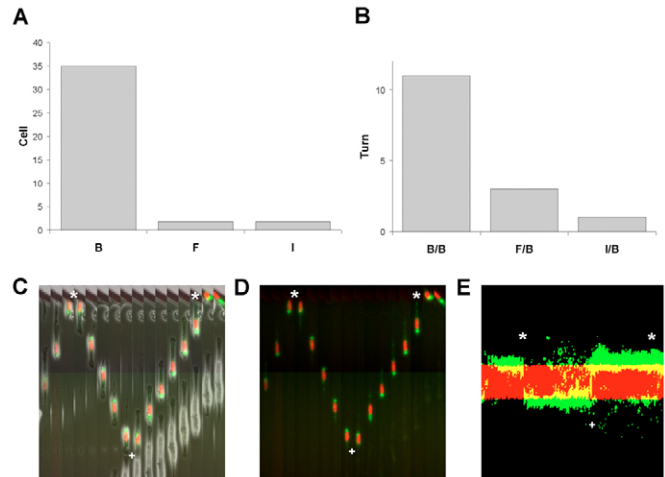


**Fig. 4.** The position of the Golgi is constant. (A) The position of the Golgi complex in Bsc1 cells grown on 6- $\mu\text{m}$  fibronectin lines (B, back; I, intermediate; F, front). (B) The position of the Golgi complex in Bsc1 cells grown on 6- $\mu\text{m}$  fibronectin lines after reorientation of the migration direction (B/B, initial back position and final back position; I/B, initial intermediate position and final back position; F/B, initial front position and final back position). (C) Sequence of the reorientation of the motility direction of a Bsc1 cell, Golgi (green), nucleus (red). Changes of direction are indicated by asterisks (\*) when the cell reaches the coverslip border, and by a plus sign (+) when the cell encounters another cell. (D) Same as C omitting the transmission channel. (E) Kymograph of the complete sequence shown in C, centered on the nucleus (red). The Golgi complex is shown in green.

location of the Golgi complex is maintained by an active mechanism and not by a random distribution on either side of the nucleus during spreading.

#### The position of the Golgi complex is linked to the position of the MTOC

Many studies have pointed out a major role for the MTOC in Golgi positioning (Thyberg and Moskalewski, 1999). We therefore investigated whether centrosome always colocalizes with the Golgi complex when the latter is behind the nucleus. Using immunofluorescence, we show that the centrosome always colocalizes with the Golgi complex on linear patterned cells (Fig. 5A-E). We also transfected cells with a Centrin-GFP plasmid to follow the position of the MTOC and the Golgi complex during migration and turns. As shown in Fig. 5F, the MTOC (thin arrows) is located at the rear during migration (large arrows indicate the direction) and relocates at the same time as the Golgi complex at the back of the cell when it turns (supplementary material Movie 4). This shows that both the Golgi complex and the MTOC colocalize at the rear of cells that migrate on linear patterns, and relocate to the new rear of the cells when the direction of migration is changed.

**Table 2.** Positions of the Golgi complex (in %) in migrating cells grown under a number of patterned growth conditions

|        | 6 $\mu\text{m}$ , plain | 14 $\mu\text{m}$ , plain | 20 $\mu\text{m}$ , plain | 23 $\mu\text{m}$ , 2 lines | 25 $\mu\text{m}$ , plain | 30 $\mu\text{m}$ , plain | 40 $\mu\text{m}$ , 3 lines | 40 $\mu\text{m}$ , plain |
|--------|-------------------------|--------------------------|--------------------------|----------------------------|--------------------------|--------------------------|----------------------------|--------------------------|
| Front  | 20 (53)                 | 15 (34)                  | 29 (24)                  | 42 (130)                   | 21 (28)                  | 30 (49)                  | 50 (70)                    | 45 (47)                  |
| Middle | 10 (53)                 | 20 (34)                  | 8.5 (24)                 | 16 (130)                   | 39.5 (28)                | 40 (49)                  | 20 (70)                    | 25 (47)                  |
| Back   | 70 (53)                 | 65 (34)                  | 62.5 (24)                | 42 (130)                   | 39.5 (28)                | 30 (49)                  | 30 (70)                    | 30 (47)                  |

Numbers in parentheses give the numbers of total cells.

### The Golgi complex is at the rear of migrating cells in the zebrafish lateral line

Since our system can only account partially for in vivo 3D geometrical constraints, we then wanted to know whether the Golgi complex can also localize at the rear in 3D cells that migrate in vivo. We therefore took advantage of a well-established model system, the zebrafish lateral line primordium (llp) (Ghysen and Dambly-Chaudière, 2007). The zebrafish llp is a tissue comprised of about 100 cells that migrate in an orchestrated manner from the head of the embryo to the tip of its tail in about 24 hours. The migration takes place along a thin strip of the chemokine Sdf1a and depends on the presence of the two chemokine receptors Cxcr4 and Cxcr7 in the front and the back of the primordium, respectively (Fig. 6A,B). The strip of Sdf1a, in addition to provide directional information, is likely to geometrically constrain the tissue. We evaluated this constraint by measuring the width of the primordium and the number of cells at the tip of the tissue. The primordium has an average of  $2 \pm 0.5$  cells in front and a width of  $15 \pm 3.9 \mu\text{m}$ . This system presents therefore similarities with cells that migrate on micropatterns.

We injected mRNA that encodes one of the two Golgi markers p115 and GM130 fused to the GFP together with a lynTdtomato RNA to label the cell membranes. The position of the Golgi complex in the primordium was consistent with that of both markers (Fig. 6D-F). Interestingly, in the dynamically migrating leading region, the Golgi complex was localized in the most apical and posterior part of the cells relative to the direction of migration, abutting the posterior part of the cell membrane (Fig. 6E,F). In addition, the centrosomes were also always localized apically and behind the nucleus in the front cells (Fig. 6G). Electron microscopy analyses confirmed that Golgi and centrosomes are close together – apical to the nucleus – throughout the primordium (Fig. 6H,K-N). In particular in the front cell, the Golgi complex was observed to abut the posterior part of the plasma membrane (Fig. 6I,J,O). Altogether, this indicates that, similar as for cells migrating on linear micropatterns under geometrical constraints, the Golgi complex and the centrosome localize behind the nucleus in cells that migrate in a constraint environment in vivo.

### Discussion

Although a subject of considerable study, the causal relationship between cell polarization, cell locomotion and the positioning of the Golgi complex has remained unclear (Schaar and Mc Connell, 2005; Yvon et al., 2002; Danowski et al., 2001). Using micro contact printing ( $\mu\text{CP}$ ), we established an in-vitro system to reproduce tracks of adhesive proteins (fibronectin) that partially mimic the constrained environment cells develop in, to analyse the positions of the Golgi complex and the centrosome.

#### Polarization of cells and organelles along lines of fibronectin

In vivo, cells evolve in a highly ordered and constrained environment. Cell migration under such conditions is guided by extracellular cues: soluble factors or physical factors. The

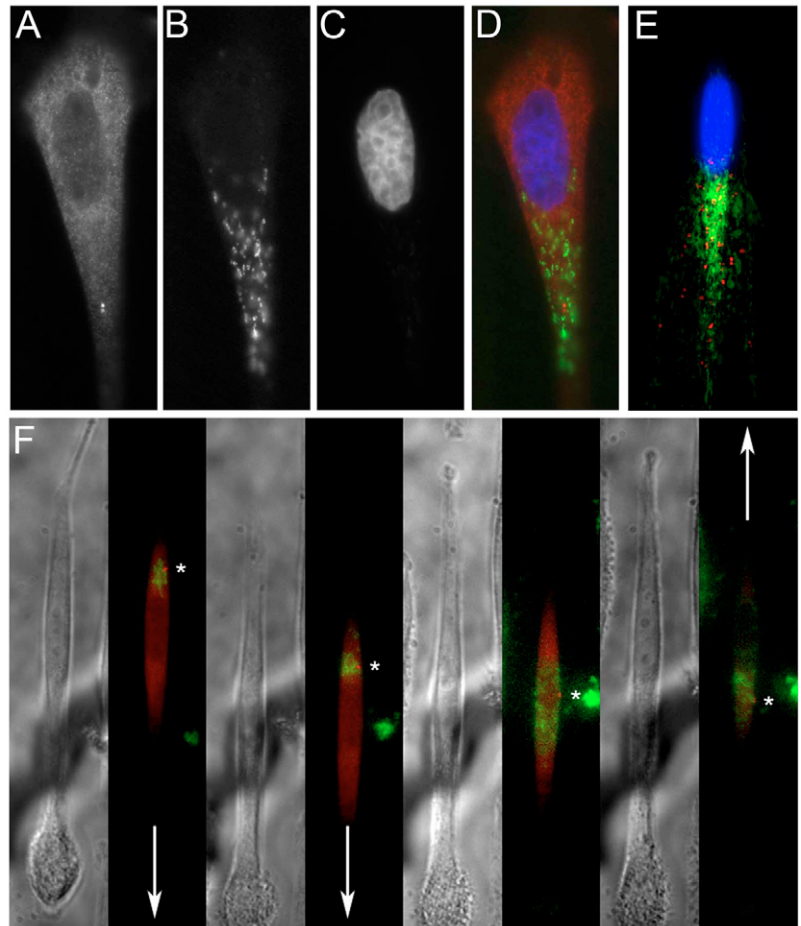


**Fig. 5.** The MTOC and the Golgi complex are moved to the new rear upon direction changes. (A-C) Staining of Bsc1 cells for (A)  $\gamma$ -tubulin (centrosomal protein), (B) GM130 (Golgi matrix protein), (C) nucleus (Hoechst staining). (D) Overlay of A-C. (E) Projection of 25 Bsc1 cells as described in supplementary material Fig. S1 for  $\gamma$ -tubulin (red), GM130 (green) and the nucleus (blue). (F) Sequence of the reorientation of a Bsc1 cell. Shown in alternation are transmission images and immunofluorescence images of the GalT-GFP signal (Golgi matrix protein, green) and the  $\gamma$ -tubulin cherry (Gtub-cherry) highlighting the centrosome position (red) taken at 0.5 frames/hour. Direction is indicated by arrows. Centrosome position is highlighted by asterisks.

topography of the substratum has a fundamental role in the regulation of cell migration and directionality. In a process known as contact guidance, ECM fibres can be spatially arranged as to facilitate cell polarization and then movement in a preferred direction (Abrams et al., 2000). Recent advances in microfabrication techniques have demonstrated that these topographical cues can be reproduced in vitro (Chou et al., 1995; Poole et al., 2005).  $\mu\text{CP}$ , on the basis of previous studies (Xia and Whitesides, 1998; Levina et al., 2001; Brock et al., 2003), represents a compelling approach to perform a micrometer-scale patterning to control cell shape, polarization and migration. Using  $\mu\text{CP}$ , we created linear fibronectin patterns mimicking tracks of adhesive proteins found in living tissue and reproducing partially in vitro the constrained environment cells evolve in. We demonstrate that cells cultured on these substrata are polarized and geometrically constrained (Table 1). The cells but also the nuclei elongate while the Golgi complex segregate on either side of the nucleus. We also observe a parallel alignment of actin fibers

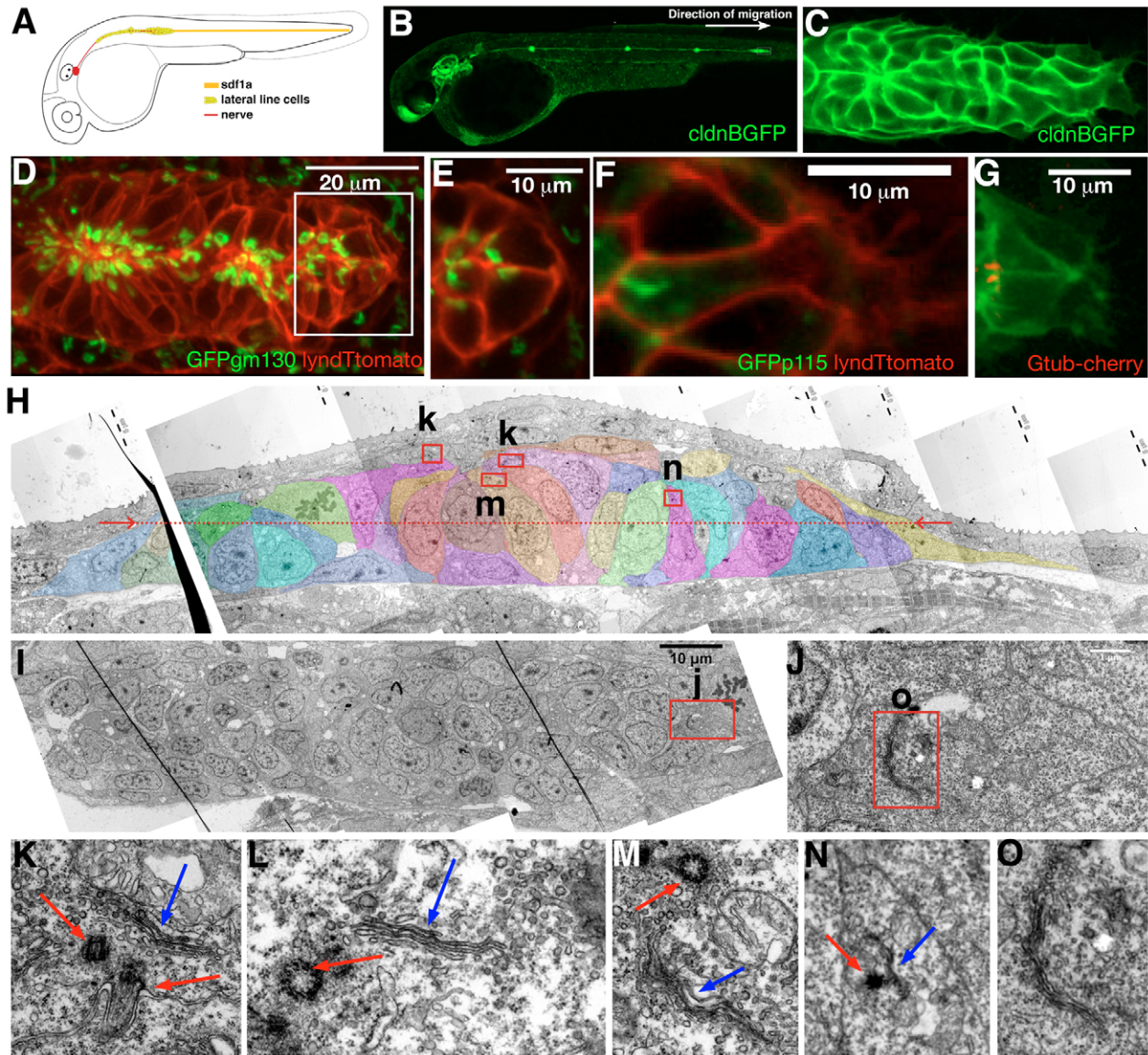


**Fig. 6.** Golgi location in the zebrafish lateral line primordium (llp). (A) Scheme of the migrating llp on the Sdf1a strip. (B) Side view of a claudinB-GFP transgenic embryo at 42 hours post fertilization (hpf) showing an overview of the posterior lateral line. (C) Magnification of the inset in A showing that many cells in the group display cellular lamellipod-like extensions in the direction of migration. (D) Side view of the llp of a zebrafish embryo expressing *gfp-gm130* (green) and *lyndTomato* (red). (E) Detailed view of the inset in D. (F) Front cell of the primordium in an embryo expressing *gfp-p115* (green) and *lyndTomato* (red) showing the Golgi in the most posterior part of the cell. (G) Front cells of the primordium in a *CldnB:GFP* embryo with  $\gamma$ -tubulin cherry (*Gtub-cherry*) highlighting the centrosome position. (H,K-N) TEM micrographs of a parasagittal section of a 40 hpf primordium. (H) Assembly of 12 images showing a side view across most of the primordium. Cells have been pseudo-coloured and insets are magnified below (k,l,m,n). (I) Longitudinal section of the primordium as represented by the arrows in H. The section goes through all the nuclei except in the front-most cell, which is slightly flatter. (J) Detailed view of the front-cell inset in I showing the Golgi complex abutting the plasma membrane in the back. (O) Inset from J magnified, showing a detailed view of the Golgi complex. (K-N) Magnification of the insets indicated in H (labelled k, l, m, n) showing the close association of the Golgi complex with the centrosomes in different cells throughout the migrating tissue from the back of the primordium (K,M) to the front (L,N). Blue arrows, Golgi complex; red arrows, centrosome. Posterior is on the right and dorsal is to the top in all panels. The direction of migration is from the left to right as indicated by the arrow in B.

along the fibronectin line axis as well as mitochondria and microtubules (Fig. 1C,D and data not shown). This is in agreement with previous studies showing that focal adhesions, actin microfilaments bundles (Teixeira et al., 2003) and microtubules (Oakley et al., 1997) align along the microstructures they grow on, while not showing any preferred orientations when grown on flat uniform glass substrates. This could explain why cell migration is oriented along the fibronectin line axis by simple orientation

of the cytoskeleton, and as a consequence of the attachment points and the traction forces. Moreover, the alignment of the cytoskeleton could explain the nuclear shape and the segregation of the Golgi complex on one side (Fig. 1C and Fig. 2F). In the case of Bsc1 cells, the width of the nucleus is almost the same as that of the line (Table 1). Such geometrical organization de facto generates a front and a rear part of the cell that are separated by the nucleus. This suggests that the polarized distribution of

organelles in the cytoplasm is spatially coupled with structural and functional polarity, as observed in migrating T lymphocytes (Ratner et al., 1997).

#### Polarization and displacement of the Golgi complex

We observed that not only is the Golgi complex segregated to either side of the nucleus because of geometrical constraints but it is also displaced up to 20  $\mu\text{m}$  away from the nucleus in patterned cells. Such a displacement of the Golgi complex from its usual juxtannuclear localization during cell migration has never been reported in the literature for migrating cells *in vitro*. Interestingly, migrating neurons *in vivo* developed dilations within the leading process that were ahead of the nucleus, and contained the centrosome and membrane vesicles that can be moved several micrometres before (Schaar and McConnell, 2005) (Fig. 7B). This is owing to the nucleokinesis process that is believed to occur in two alternating phases: (1) forward migration of the Golgi and/or the centrosome that are associated with centrosome splitting and, (2) myosin contraction at the rear (Schaar, 2005). We observed exactly the opposite when the Golgi complex was displaced towards the rear during cell migration. As the Golgi complex always localized with the centrosome (Fig. 5) (Thyberg and Moskalewski, 1999), this migration-dependent displacement could be explained by an initial nucleokinesis phase – in which the centrosome pushes the nucleus ahead (Dogterom et al., 2005) – in coordination with a myosin-based nuclear movement as demonstrated previously (Gomes et al., 2005). The Golgi complex is positioned through microtubule-linked motors (Caviston and Holzbaur, 2006) and, therefore, follows the centrosomal relocation. This leads to a displacement of the Golgi complex from its juxtannuclear localization before the relocation of the centrosome to a position that is closer to the nucleus when the rear adhesion points are released as part of the migration process.

#### Positioning of the Golgi complex and directional cell migration

Cell migration on linear patterns leads to a rear location of the Golgi complex (Fig. 7B,F), whereas it has been shown that, during cell migration, the Golgi complex preferentially localizes to the leading edge (Etienne-Manneville, 2004) (Fig. 7A,E). In this work, we confirm that the geometrical constraints induced by the substratum determine the position of the Golgi complex (Table 2). Its anterior position in Bsc1 cells increases from 20% to 45% with the width, whereas the rear position decreases from 70% cells to a minimum of 30% cells as the width increases. We assumed in our study that the Golgi complex always localized with the centrosome, as shown in Fig. 5. In a wound-healing assay, for which cells are released from constraints by scratching the cell monolayer, Euteneuer and Schliwa observed that the centrosome position is anterior for 40% of the cells 30 minutes after wounding, and up to  $80\pm 5\%$  after 3 hours, which translates to a posterior position in 60% and 20% of the cells, respectively (Euteneuer and Schliwa, 1992). Yvon et al. showed, by using a similar assay, that Chinese hamster ovary (CHO) cells have an anterior position in 29% of the cells, which increases to 73.2% 4 hours after wound healing (Yvon et al., 2002). Another study observed that cells that migrate from a plaque on glass or on gels have an anterior MTOC at 73% or 45.4%, respectively and, so, a posterior position in 27% or 54.6%, respectively (Schütze et al., 1991). Our results explain these previous observations, and we show that cells under constraints display a preferential rear location of the centrosome and/or the Golgi complex. We conclude that relocation to the front is not only due to the polarization and the

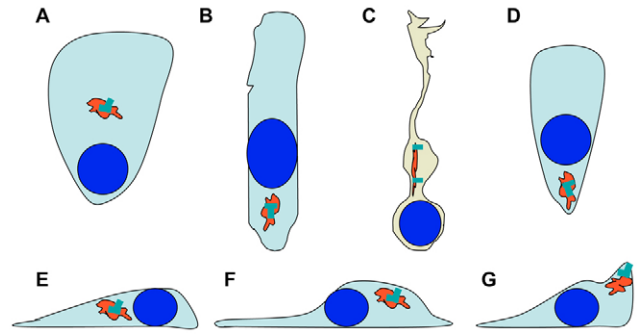


**Fig. 7.** Cell migration models. (A) Top view of a migrating cell on a glass substrate. (B) Top view of a migrating cell on linear FN pattern. (C) Top view of a migrating neuron. (D) Top view of a migrating T lymphocyte. (E) Side view of a migrating cell on a glass substrate. (F) Side view of a migrating cell on linear FN pattern. (G) Side view of a migrating T lymphocyte.

migration of the cell but rather by the fact that the geometrical constraints are removed, as is the case in a wound-healing assay (Yvon et al., 2002) or when a cell moves out of an explant (Euteneuer and Schliwa, 1992). However, it is often assumed that a migrating cell has a large leading edge. This maybe true because cells that migrate on glass surfaces are free to expand in any direction unlike cells that migrating *in vivo*. Other researcher that have used  $\mu\text{CP}$  even assumed that a migrating cell must have a large leading edge (Jiang et al., 2005) and have used asymmetric patterns to force cell shape. Such an experimental set-up would lead to a forced migration towards the larger end of the cell and a front position of the Golgi complex. Our experiments do not support such conclusions, because a simple linear geometrical constraint reduces the leading edge and automatically places the Golgi complex and centrosome at the rear end of the cells, without affecting their migration behaviour. Moreover, we observed a similar position of the Golgi complex in the leading cells of the zebrafish lp. Our observations therefore indicate that the presence of the Golgi complex and the MTOC in front of a migrating cell is not crucial for migration. It has been proposed that Cdc42 and the positioning of the Golgi and MTOC in the front have a crucial role in directed migration (Itoh et al., 2002). However, fibroblasts that are devoid of a functional Cdc42 gene still polarize normally (Czuchra et al., 2005) and we observed that, in our system, Cdc42 is found on the Golgi complex at the rear but also at the leading edge (data not shown). This indicates that even a rear position of the Golgi complex and the MTOC do not affect the functionality of known effectors of migration. It seems clear that the geometrical constraints, which are even higher *in vivo*, affect the intracellular organization and possibly lead to a 'leukocyte-like' organization of the Golgi complex near the MTOC, which is localized in a uropod-like structure. It is conceivable that actin is the main player during the migration process in such a dense environment, in which geometrical constraints are important and the tracks on which the cells migrate are narrow. It is well-established that adhesion complexes are linked to the actin cytoskeleton (Sastry and Burrridge, 2000) and that changes in actomyosin contractility can alter adhesive contacts (Chrzanowska-Wodnicka and Burrridge, 1996; Katz et al., 2000). Recent experiments further show that microtubules can target focal adhesions and that expression of cadherin can regulate the dynamic behaviour of microtubules (Kaverina et al., 1999). Adhesion could

directly influence the position of microtubules, centrosomes and the Golgi complex. Alternatively, microtubule behaviour could be altered indirectly by changes in contractility. This latter possibility is supported by the observation that the activity of actomyosin modulates the organization, turnover and motion of microtubules in mammalian cells (Yvon et al., 2001).

### Functions of the Golgi complex and the MTOC during directional cell migration

By simply constraining cells, our system leads to a rear location of the Golgi complex and the centrosome during migration. Our assay allows the reproduction of the migration behaviour observed in vivo for T-lymphocyte (Fig. 7G) or the leading cells of the zebrafish lateral line (Fig. 6). Our study demonstrates that geometrical constraints are a very important factor that determines the Golgi complex and centrosome positions within a cell during migration.

## Materials and Methods

### Antibodies and reagents

All cell culture media and sera were obtained from Invitrogen. Plasmids encoding GFP-p115 and GFP-GM130 were a kind gift from Francis Barr (University of Liverpool, UK). The centrin-GFP was kindly provided by Annie Rousselet (Institut Curie, Paris). The following antibodies were used: monoclonal GM130 antibody (BD Biosciences),  $\gamma$ -tubulin, Alexa-Fluor-488-conjugated phalloidin (Molecular Probes). Reagents were fibronectin (Sigma-Aldrich), fibrinogen Alexa-Fluor-647 (Molecular Probes), tricaine (Sigma), mMessage mMachine kit (Ambion).

### Cell culture

Vero, Ptk2 and Bsc1 cells were cultured in Dulbecco's modified Eagle's medium (DMEM, Life Technologies, Karlsruhe, Germany) supplemented with 10% foetal calf serum (FCS), streptomycin (100 U/ml and 100  $\mu$ g/ml, respectively) at 37°C in 5% CO<sub>2</sub>. Cells were spread on patterned surfaces or on live cell dishes (MatTek Corp., Ashland, MA) at a density of ~15,000 cells/ml. 24 hours later cells were transfected with expression constructs (0.6  $\mu$ g each) using per dish 2.6  $\mu$ l of FuGene6 Transfection Reagent (Roche, Indianapolis, IN). Cells were imaged 12 hours after transfection.

### Immunofluorescence

Cells were stained and mounted on glass slides as previously described (Reynaud et al., 2005). In brief, cells were fixed with 4% paraformaldehyde in PBS, blocked in 50 mM NH<sub>4</sub>Cl in PBS, permeabilized in 0.1% Triton X-100 in PBS and stained with Alexa-Fluor-488-conjugated phalloidin or the appropriate antibodies. When observing the motility of patterned cells, cells were fixed 12 hours after plating and labelled with Alexa-Fluor-488-conjugated phalloidin.

### Patterning techniques and coverslip mounting

The layout design of the stamp used in this work was done using CleWin Software (WieWeb, Hengelo, The Netherlands). The design was first translated into 5-inch chromium photolithography masks by Delta Mask V.O.F. (Enschede, The Netherlands), which was subsequently used to produce a structured silicon master (3  $\mu$ m depth) using a positive tone-resist process. Poly(dimethylsiloxane) (PDMS) stamps were fabricated by curing Sylgard 184 (Dow Corning, Midland, MI) onto this fluorinated silicon master at 60°C for 24 hours in an oven. After curing, the elastomer was peeled off from the master revealing the pre-designed three dimensional surface structures of the stamp.

Prior to any surface modifications, the glass coverslips (15 mm in diameter; Menzel Gläser, Braunschweig, Germany) were first washed in acetone and ethanol, then rinsed in deionized water and dried under flow of nitrogen gas. In all experiments, the PDMS stamps were incubated with an 100  $\mu$ l aliquot of a 1:2 mixture of fibronectin and fibrinogen Alexa-Fluor-647 solution at a final protein concentration of 50  $\mu$ g/ml in 1  $\times$  PBS for 30 minutes. The stamps were then washed in deionized water and blow-dried in a stream of nitrogen (FN-stamp).

For a faster and efficient silanization, the cleaned glass slides were treated for 1 minute with oxygen plasma (PlasmaPrep2, Structure Probe, West Chester, PA) before silanization. Silanization of the slides was performed by immersing them in 5% 3-aminopropyltriethoxysilane (APTS) acetone solution for 30 seconds followed by several washing steps in 1  $\times$  PBS. The slides were then incubated in ~0.5 mg/ml bis(sulfosuccinimidyl) suberate in 1  $\times$  PBS (BS3 Sigma-Aldrich) for 10 minutes. Blow-dried FN stamps as described above were then placed in contact with silanized glass surfaces for 5 minutes. After removal of the stamp, the slides were incubated as for non-covalent approach in a 1 mg/ml poly(L-lysine)-g-poly(ethylene glycol) (PLL-g-PEG) for 30 minutes for back-fill. All these processes were done at room temperature.

The patterned glass slides were attached to 10-mm holes at the bottom of 35-mm plastic Petri dishes using silicon-free grease (Glisseal N, Borer Chemie, Jesteburg, Germany).

### Live imaging and measurements

Bright-field and fluorescence digital images were acquired either with an Axiovert 200 inverted microscope (Zeiss, Oberkochen, Germany) or with a DeltaVision system (Applied Precision Inc., Issaquah, WA) for panel image acquisitions.

Analysis of the cell characteristics were performed as described below (see also supplementary material Fig. S1). Transmission or fluorescent images of the cells were acquired and demarcated and the cell contours were extracted. All cell contours were centred according to the centre of mass and then projected. To process and centre the cell contours, they were fitted with an ellipse allowing the calculation of the centre of mass. To allow a comparison of cell populations, cell-fitted ellipses were aligned along the major cell axis the cell contours, which allowed measurement of the major axis and minor axis of an entire cell population once the cell contours were projected. An identical approach was used to measure the characteristics of the nucleus using the nucleus instead of the cell contours for the analysis process. The deformation index (DI) is defined as 'major minus minor' divided by 'major plus minor', a value of DI=0 describes a circle.

The distance between the Golgi complex and the nucleus was measured as follow (see also supplementary material Fig. S2). The fluorescent images of the nucleus, Golgi complex and cell membrane were acquired, demarcated and segmented. Surface and contours of the Nucleus and Golgi complex were determined and projected. The distance and angle between the border of the nucleus and every single pixel that defined the Golgi complex was measured. The results were plotted using a box-plot representation where y is the distance of the nuclear border (o) to the Golgi complex in  $\mu$ m. The box illustrates the average spreading of the Golgi as well as the maximum and minimum distance between the nuclear envelope and the Golgi complex. All steps have been implemented as a Macro for ImageJ.

The analysis of the Golgi position in regard to the direction of migration was performed in a double-blind manner by two different persons using the phalloidin channel to assess cell direction.

### mRNA injection and zebrafish imaging

The *CldnB:GFP* transgenic zebrafish line (expressing claudin B tagged with GFP) (Haas and Gilmour, 2006) was maintained and raised as described (Kimmel et al., 1995). The *LynGFP* is under the control of the claudin B promoter. To label the Golgi complex in living embryos, GFP-p115 and GFP-gm130 were subcloned into the pCS2+ vector and mRNA synthesis was carried out using the mMessage mMachine kit (Ambion). 25 ng/ $\mu$ l of GFP-p115 or GFP-gm130 mRNAs was co-injected with 100 ng/ $\mu$ l of *lyndTtomato* mRNA in zebrafish eggs at the one-cell stage. 36 hpf embryos were anesthetized with 0.01% tricaine and embedded in 1.5% low-melting-point agarose. Time-lapse analysis was carried out on an Olympus Fluoview 1000 using a 60 $\times$ /NA 1.2 water objective and the 488 nm and 566 nm laserlines. The overview image was taken using a 10 $\times$ /NA 0.3 objective. Ten z-stacks spanning ~10  $\mu$ m were captured. Projections were carried out using maximum projection plugin of ImageJ software.

### Electron microscopy

Images of 40 hpf whole-mount *CldnB:GFP* transgenic embryos (Haas and Gilmour, 2006) were first taken under a fluorescent compound microscope before dissecting a small section of trunk that contained both lateral line primordia. These regions were individually fixed (6% glutaraldehyde in 0.1 M cacodylate buffer) for 30 minutes at room temperature, washed in 50  $\mu$ M cacodylate buffer (five times for 5 minutes) and kept at 4°C. They were then postfixed in 2% osmium tetroxide for 1 hour on ice, washed in water (three times for 5 minutes), contrasted with 0.5% uranylacetate overnight at 4°C and washed in water (five times for 5 minutes). Finally, te regions were dehydrated in a graded series of ethanol, equilibrated in a 1:1 mixture of propyleneoxide:Epon for 4 hours or overnight at room temperature. They were then washed twice with Epon and infiltrated in Epon for 4-6 hours at room temperature, flat embedded and baked for 48 hours at 65°C. Ultrathin sections (60 nm thick) were cut on an Ultracut microtome (Leica Microsystems) and stained using the Pelco Grid staining system (EMS).

Plasmids encoding GFP-p115 and GFP-GM130 were a kind gift from Francis Barr (University of Liverpool, UK). The Centrin-GFP plasmid was kindly provided by Annie Rousselet (Institut Curie, Paris, France). We thank the members of the Advanced Light Microscopy Core Facility (ALMF) for their help during this project. We thank the reviewers for their critical readings and comments.

## References

- Abrams, G. A., Goodman, S. L., Nealey, P. F., Franco, M. and Murphy, C. J. (2000). Nanoscale topography of the basement membrane underlying the corneal epithelium of the rhesus macaque. *Cell Tissue Res.* **299**, 39-46.

- Anstrom, J. A. and Raff, R. A. (1988). Sea urchin primary mesenchyme cells: relation of cell polarity to the epithelial-mesenchymal transformation. *Dev. Biol.* **130**, 57-66.
- Brock, A., Chang, E., Ho, C. C., LeDuc, P., Jiang, X., Whitesides, G. M. and Ingber, D. E. (2003). Geometric determinants of directional cell motility revealed using microcontact printing. *Langmuir*, **19**, 1611-1617.
- Carney, P. R. and Couve, E. (1989). Cell polarity changes and migration during early development of the avian peripheral auditory system. *Anat. Rec.* **225**, 156-164.
- Caviston, J. P. and Holzbaur, E. L. (2006). Microtubule motors at the intersection of trafficking and transport. *Trends Cell Biol.* **16**, 530-537.
- Chou, L., Firth, J. D., Uitto, V. J. and Brunette, D. M. (1995). Substratum surface topography alters cell shape and regulates fibronectin mRNA level, mRNA stability, secretion and assembly in human fibroblasts. *J. Cell Sci.* **108**, 1563-1573.
- Chrzanoska-Wodnicka, M. and Burridge, K. (1996). Rho-stimulated contractility drives the formation of stress fibers and focal adhesions. *J. Cell Biol.* **133**, 1403-1415.
- Coan, D. E., Wechezak, A. R., Viggers, R. F. and Sauvage, L. R. (1993). Effect of shear stress upon localization of the Golgi apparatus and microtubule organizing center in isolated cultured endothelial cells. *J. Cell Sci.* **104**, 1145-1153.
- Czuchra, A., Wu, X., Meyer, H., van Hengel, J., Schroeder, T., Geffers, R., Rottner, K. and Brakebusch, C. (2005). Cdc42 is not essential for filopodium formation, directed migration, cell polarization, and mitosis in fibroblastoid cells. *Mol. Biol. Cell* **16**, 4473-484.
- Danowski, B. A., Khodjakov, A. and Wadsworth, P. (2001). Centrosome behavior in motile HGF-treated PtK2 cells expressing GFP-gamma tubulin. *Cell Motil. Cytoskeleton* **50**, 59-68.
- Dogterom, M., Kerssemakers, J. W., Romet-Lemonne, G. and Janson, M. E. (2005). Force generation by dynamic microtubules. *Curr. Opin. Cell Biol.* **17**, 67-74.
- Dunn, G. A. (1983). Characterising a kinesis response: time averaged measures of cell speed and directional persistence. *Agents Actions Suppl.* **12**, 14-33.
- Etienne-Manneville, S. (2004). Cdc42 – the centre of polarity. *J. Cell Sci.* **117**, 1291-1300.
- Etienne-Manneville, S. and Hall, A. (2002). Rho GTPases in cell biology. *Nature* **420**, 629-635.
- Euteneuer, U. and Schliwa, M. (1992). Mechanism of centrosome positioning during the wound response in BSC-1 cells. *J. Cell Biol.* **116**, 157-166.
- Gail, M. H. and Boone C. W. (1970). The locomotion of mouse fibroblasts in tissue culture. *Biophys. J.* **10**, 980-993.
- Ghysen, A. and Dambly-Chaudière, C. (2007). The lateral line microcosmos. *Genes Dev.* **21**, 2118-2130.
- Gomes, E. R., Jani, S. and Gundersen, G. G. (2005). Nuclear movement regulated by Cdc42, MRCK, myosin, and actin flow establishes MTOC polarization in migrating cells. *Cell* **121**, 451-463.
- Haas, P. and Gilmour, D. (2006). Chemokine signaling mediates self-organizing tissue migration in the zebrafish lateral line. *Dev. Cell* **10**, 673-680.
- Itoh, R. E., Kurokawa, K., Ohba, Y., Yoshizaki, H., Mochizuki, N. and Matsuda, M. (2002). Activation of Rac and Cdc42 video imaged by fluorescent resonance energy transfer-based single-molecule probes in the membrane of living cells. *Mol. Cell Biol.* **22**, 6582-6591.
- Jiang, X., Bruzewicz, D. A., Wong, A. P., Piel, M. and Whitesides, G. M. (2005). Directing cell migration with asymmetric micropatterns. *Proc. Natl. Acad. Sci. USA* **102**, 975-958.
- Katz, B. Z., Zamir, E., Bershadsky, A., Kam, Z., Yamada, K. M. and Geiger, B. (2000). Physical state of the extracellular matrix regulates the structure and molecular composition of cell-matrix adhesions. *Mol. Biol. Cell* **11**, 1047-1060.
- Kaverina, I., Krylyshkina, O. and Small, J. V. (1999). Microtubule targeting of substrate contacts promotes their relaxation and dissociation. *J. Cell Biol.* **146**, 1033-1044.
- Kimmel, C. B., Ballard, W. W., Kimmel, S. R., Ullmann, B. and Schilling, T. F. (1995). Stages of embryonic development of the zebrafish. *Dev. Dyn.* **203**, 253-310.
- Kupfer, A., Louvard, D. and Singer, S. J. (1982). Polarization of the Golgi apparatus and the microtubule-organizing center in cultured fibroblasts at the edge of an experimental wound. *Proc. Natl. Acad. Sci. USA* **79**, 2603-2607.
- Lehnert, D., Wehrle-Haller, B., David, C., Weiland, U., Ballestrem, C., Imhof, B. A. and Bastmeyer, M. (2004). Cell behaviour on micropatterned substrata: limits of extracellular matrix geometry for spreading and adhesion. *J. Cell Sci.* **117**, 41-52.
- Levina, E. M., Kharitonova, M. A., Rovinsky, Y. A. and Vasiliev, J. M. (2001). Cytoskeletal control of fibroblast length: experiments with linear strips of substrate. *J. Cell Sci.* **114**, 4335-4341.
- Li, S., Guan, J.-L. and Chien, S. (2005). Biochemistry and biomechanics of cell motility. *Annu. Rev. Biomed. Eng.* **7**, 105-150.
- Magdalena, J., Millard, T. H. and Machesky, L. M. (2003). Microtubule involvement in NIH 3T3 Golgi and MTOC polarity establishment. *J. Cell Sci.* **116**, 743-756.
- Nabi, I. R. (1999). The polarization of the motile cell. *J. Cell Sci.* **112**, 1803-1811.
- Nemere, I., Kupfer, A. and Singer, S. J. (1985). Reorientation of the Golgi apparatus and the microtubule-organizing center inside macrophages subjected to a chemotactic gradient. *Cell Motil.* **5**, 17-29.
- Oakley, C., Jaeger, N. A. and Brunette, D. M. (1997). Sensitivity of fibroblasts and their cytoskeletons to substratum topographies: topographic guidance and topographic compensation by micromachined grooves of different dimensions. *Exp. Cell Res.* **234**, 413-424.
- Othmer, H. G., Dunbar, S. R. and Alt, W. (1988). Models of dispersal in biological systems. *J. Math. Biol.* **26**, 263-298.
- Parker, K. K., Brock, A. L., Brangwynne, C., Mannix, R. J., Wang, N., Ostuni, E., Geisse, N. A., Adams, J. C., Whitesides, G. M. and Ingber, D. E. (2002). Directional control of lamellipodia extension by constraining cell shape and orienting cell tractional forces. *FASEB J.* **16**, 1195-1204.
- Poole, K., Khairy, K., Friedrichs, J., Franz, C., Cisneros, D. A., Howard, J. and Mueller, D. (2005). Molecular-scale topographic cues induce the orientation and directional movement of fibroblasts on two-dimensional collagen surfaces. *J. Mol. Biol.* **349**, 380-386.
- Pu, J. and Zhao, M. (2005). Golgi polarization in a strong electric field. *J. Cell Sci.* **118**, 1117-1128.
- Ratner, S., Sherrod, W. S. and Lichlyter, D. (1997). Microtubule retraction into the uropod and its role in T cell polarization and motility. *J. Immunol.* **159**, 1063-1067.
- Reynaud, E. G., Andrade, M. A., Bonneau, F., Ly, T. B., Knop, M., Scheffzek, K. and Pepperkok, R. (2005). Human Lsg1 defines a family of essential GTPases that correlates with the evolution of compartmentalization. *BMC Biol.* **3**, 21.
- Sastry, S. K. and Burridge, K. (2000). Focal adhesions: a nexus for intracellular signaling and cytoskeletal dynamics. *Exp. Cell Res.* **261**, 25-36.
- Schaar, B. T. and McConnell, S. K. (2005). Cytoskeletal coordination during neuronal migration. *Proc. Natl. Acad. Sci. USA* **102**, 13652-13657.
- Schütze, K., Maniotis, A. and Schliwa, M. (1991). The position of the microtubule-organizing center in directionally migrating fibroblasts depends on the nature of the substratum. *Proc. Natl. Acad. Sci. USA* **88**, 8367-8371.
- Serrador, J. M., Nieto, M. and Sanchez-Madrid, F. (1999). Cytoskeletal rearrangement during migration and activation of T lymphocytes. *Trends Cell Biol.* **9**, 228-233.
- Teixeira, A. L., Abrams, G. A., Bertics, P. J., Murphy, C. J. and Nealey, P. F. (2003). Epithelial contact guidance on well-defined micro- and nanostructured substrates. *J. Cell Sci.* **116**, 1881-1892.
- Thyberg, J. and Moskalewski, S. (1999). Role of microtubules in the organization of the Golgi complex. *Exp. Cell Res.* **246**, 263-279.
- Xia, Y. and Whitesides, G. M. (1998). Soft lithography. *Angew. Chem. Int. Ed.* **37**, 550-575.
- Yu, W., O'Brien, L. E., Wang, F., Bourne, H., Mostov, K. E. and Zegers, M. M. (2003). Hepatocyte growth factor switches orientation of polarity and mode of movement during morphogenesis of multicellular epithelial structures. *Mol. Biol. Cell* **14**, 748-763.
- Yvon, A. M., Walker, J. W., Danowski, B., Fagerstrom, C., Khodjakov, A. and Wadsworth, P. (2002). Centrosome reorientation in wound-edge cells is cell type specific. *Mol. Biol. Cell* **13**, 1871-1880.

### Question 1

Résumé (5 points) Mots-Clés (1 point)

1 point : **In vivo**, les cellules effectuent leur migration dans un **environnement en 3 dimensions** dans lequel elles subissent des **contraintes physiques**. Cependant, les études sur la migration cellulaire ont été réalisées dans la plupart des cas en **culture sur des substrats en 2 dimensions**.

1 point : Dans les conditions de substrat en 2 dimensions, il a été montré que l'appareil de **Golgi** est localisé dans la direction **du front migratoire** de la cellule, suggérant un **rôle** dans la **migration directionnelle**.

1 point Les auteurs ont utilisé une méthode d'impression par microcontact pour produire des microstructures permettant d'étudier la migration de **cellules soumises à des contraintes géométriques affectant leur forme**. Les cellules migrant sur une microstructure consistant en une ligne de fibronectine, une molécule de la matrice extracellulaire, sont **polarisées** et **migrent dans la même direction**. **Dans ces conditions, l'appareil de Golgi, le centrosome et le MTOC sont situés à l'arrière du noyau**. De plus, le complexe de Golgi se trouve souvent à une distance du noyau de plusieurs microns.

1 point : Pour déterminer si ce positionnement du complexe de Golgi s'observait également dans l'**organisme**, les auteurs ont utilisé comme modèle l'ébauche de la ligne latérale chez le poisson zèbre, pour observer une migration dans un **environnement physiologique en 3D** et exerçant des contraintes **physiques** sur les cellules. Dans ce système, les auteurs ont observé également une **localisation à l'arrière du noyau de l'appareil de Golgi et du centrosome** dans les cellules « leader ».

1 point : L'ensemble des résultats conduit à proposer que le positionnement de l'appareil de Golgi et du centrosome est dépendant des contraintes géométriques subies par les cellules et que leur position ne serait pas reliée à une fonction dans le contrôle de la direction de migration.

5 Mots Clés (1 point)

polarité, polarisation, contraintes physiques ou géométriques, complexe de Golgi, MTOC, migration directionnelle, matrice extracellulaire, microstructure

### Question 2

Représentez en schéma et décrivez le mécanisme par lequel la fibronectine exerce ses effets (2 points)

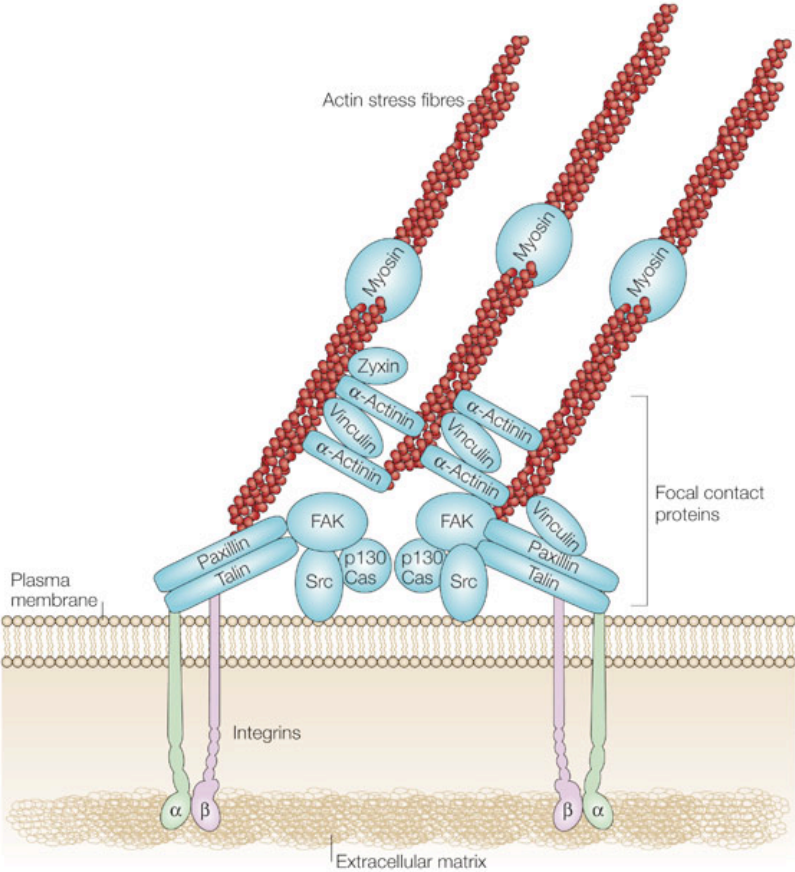
1 point

Les éléments de la matrice extracellulaire sont reconnus par les récepteurs hétérodimériques transmembranaires de la famille des intégrines.

La fibronectine est reconnue principalement par l'intégrine  $\alpha 5 \beta 1$ , mais il existe plusieurs autres intégrines qui reconnaissent la fibronectine ( $\alpha 4 \beta 1$ ,  $\alpha v \beta$ ). Le domaine extracellulaire des intégrines se lie à une séquence RGD sur la fibronectine. Le domaine cytoplasmique des intégrines se lie à des molécules cytoplasmiques (taline, vinculine,  $\alpha$ -actinine) qui vont lier les filaments d'actine. Ainsi, il existe un lien entre fibronectine et cytosquelette d'actine. Lors

de la migration, il y a formation de jonctions à l'avant (front de migration), et dissolution des contacts à l'arrière, parallèlement à la polymérisation de l'actine. Ceci permet le mouvement cellulaire.

Schéma 1 point : Figure présentée dans le cours.



### *Question 3*

*Décrivez les principaux résultats et conclusions de la figure 1 (masqués dans cette version) (3 points).*

Les panels A-C pour les cellules Bsc1 et le panel D pour les cellules Ptk2 illustrent des exemples de cellules qui montrent une morphologie beaucoup plus allongée lorsqu'elles ont étéensemencées sur des microstructures alternant bandes de fibronectine et bandes d'un substrat non adhésif, par rapport au substrat normal non structuré. Sur la ligne de fibronectine, les 2 types cellulaires montrent un phénotype polarisé. Pour quantification, la projection des contours cellulaires a été réalisée. Par exemple, la projection de 100 contours cellulaires de cellules Bsc1 sur un substrat normal en Fig 1E fait apparaître une moyenne de la forme et de la taille des cellules. Lorsqu'on aligne les cellules selon leur axe le plus long, on peut voir une nette différence entre les cellules sur substrat normal (Fig. 1F) et cellules sur microstructures de fibronectine (Fig. 1G) qui montrent une forme très allongée. Un résultat similaire est observé avec la lignée Ptk2 (Fig. 1 H,I).

Dans les cellules polarisées Bsc1, l'appareil de Golgi est trouvé dans la plupart des cas d'un côté du noyau (à l'arrière), et parfois déplacé à distance du noyau.

De plus, non seulement les cellules, mais aussi les noyaux montrent une morphologie allongée dans le cas des Bsc1. La largeur moyenne des noyaux le long de la ligne de fibronectine, est équivalente à l'épaisseur de la ligne (Fig1J), indiquant la aussi une contrainte géométrique.

En conclusion de cette expérience, les cellulesensemencées sur une microstructure de fibronectine présentent un phénotype polarisé, une forme allongée de la cellule et du noyau causés par la contrainte géométrique imposée par la structure du substrat.

*Question 4 Quels autres marqueurs auraient pu être utilisés dans cette étude pour visualiser les zones de contact avec le substrat ? (2 points)*

Anticorps contre les composants des plaques d'adhérence : voir schéma  
Exemples : intégrines, taline, paxilline, vinculine, FAK, phosphotyrosine

*Question 5 : Qu'apporte la vidéomicroscopie (ou time-lapse) dans cette étude ? (2 points)*

La vidéomicroscopie a été utilisée pour prendre en compte les aspects de dynamique au cours du temps : pour observer si la position de l'appareil est transitoire ou permanente, et pour mettre en évidence les changements éventuels. Deux types de morphologies cellulaires ont pu être observés. L'une correspond à des cellules courtes à migration rapide, l'autre à des cellules allongées à migration lente. Les auteurs ont pu montrer que l'appareil de Golgi est à l'arrière du noyau dans 70% des cas de cellules allongées, qui migrent sur une ligne étroite de fibronectine. En revanche, si les cellules occupent plus d'une ligne ou si l'épaisseur de la ligne augmente, la position à l'arrière du noyau n'est retrouvée que dans 30% des cellules, indiquant que la forme et l'espace occupé par la cellule influe sur la position du complexe. Enfin, cette position est maintenue lors de changements de direction de la migration. La vidéomicroscopie a également été utilisée pour visualiser *in vivo* la migration des cellules de la ligne latérale.

*Question 6 : Il existe de nombreux exemples de migration cellulaire in vivo. Expliquez le choix de ce système particulier par les auteurs. Quel(s) paramètre(s) sont mieux pris en compte par rapport à la culture cellulaire ? (3 points)*

La ligne latérale du poisson zèbre est un système bien établi dans lequel une centaine de cellules migrent de façon coordonnée de la tête vers la queue de l'embryon en 24 heures. Les cellules migrent sur une fine bande de la chemokine Sdf1a et dépendent de la présence de récepteurs de surface cellulaire. Une cellule leader sert de guide aux cellules suivantes. Ce système présente des similarités avec le système de microstructures dans le fait qu'il impose des contraintes géométriques et une direction de migration. L'espace en 3D avec volume et contraintes physiques, la répartition des molécules de substrat sont mieux pris en compte dans ce système *in vivo*.

*Question 7 : Que permet de visualiser la claudine-GFP chez le poisson-zèbre ? (1 point)*

La claudine est un composant des jonctions serrées présentes au pôle apical des cellules. Dans ce cas, le transgène claudine-GFP permet de visualiser le contour des cellules de la ligne latérale. A des forts grossissements (fig. 6C) ce marquage permet de visualiser des extensions de type lamellipode dans le front des cellules en migration.

*Question 8 : Comment met-on en œuvre un test de « wound-healing » in vitro ? (1 point)*

Une culture de cellules est amenée à confluence. Sur la couche de cellules, on introduit une « blessure » en appliquant à l'aide d'un cône ou d'une lame un trait régulier, de manière à décrocher les cellules sur une ligne. Les cellules des 2 bords seront ainsi induites à migrer

pour réparer la blessure et combler l'espace. On peut suivre par videomicroscopie en contraste de phase les différents paramètres de la migration cellulaire, et comparer différentes situations expérimentales (dans le cours une cellule déficiente en intégrine comparée au sauvage).